Implementing BPL Transmission in MV Cable Network Effectively

Grzegorz Debita[1], Marcin Habrych[1], Andrzej Tomczyk[1], Bogdan Miedzinski[2], Jan Wandzio[3]

[1]*Wroclaw University of Science and Technology,*
Wybrzeze Wyspianskiego 27, 50-370 Wroclaw, Poland
[2]*Institute of Innovative Technologies EMAG,*
40-189 Katowice ul Leopolda 31, Poland
[3]*KGHM Polska Miedz S.A.*
ul M.Sklodowskiej-Curie 48,59-301 Lubin, Poland
grzegorz.debita@pwr.edu.pl

Abstract—**This paper presents and discusses the results of theoretical approach of the BPL (Broadband over Power Line: 2 MHz–32 MHz) transmission efficiency in 6 kV cable line of selected underground mine. The research verifies its validity through practical measurements. It is followed by the derivation of the power line parameters using the transmission line theory. The tests under the mine conditions were carried out for a specific 6 kV mine cable, with steel armour, for as inductive as well as capacitive coupling of BPL modems with the MV grid. The obtained results are not found so far in the literature and constitute the innovation of the achievement. On the basis of the results the conclusions for practical applications have been formulated.**

Index Terms—**Broadband over Power Line transmission (BPL); Power Line Communication (PLC); MV cable network; Underground mine; Orthogonal Frequency-Division Multiplexing (OFDM).**

I. INTRODUCTION

Transmission PLC (Power Line Communication) is an alternative to other communication systems having as their advantages and disadvantages. Its main advantage is the low cost associated with the use of existing network infrastructure [1]–[3]. The disadvantage however, is the negative impact of the environment on the range and transmission quality [1]. In the mining networks of medium voltage (over 6 kV) transmission of high frequency (BPL-Broadband over Power Line) can be successfully used both for the control and monitoring of environmental parameters and primarily as transmission of "last chance" under the mine disaster. The cable networks are the most resistant to mechanical damage and thus constitute still operating (when battery powered) transmission channel under various critical situations. However, to ensure effective PLC transmission the impact of a number of factors, such as the external (harsh environment) as well as internal, related to physical parameters and structure of a transmission line (cables, cable joints, connectors etc.) value and nature of the load current (distorted waveforms due to power converters), must be clarified and examined. It should be noted that the influence of the above factors is variable over time and can be unpredictable [4]–[6]. Depending on the bandwidth (medium and high-frequency) and the nature of the power grid (low or middle voltage) different problems become critical to overcome. For the LV power line noise, impedance, attenuation and so called bridged-tapes are found to be the three critical channel parameters [4]–[7]. Whereas, for MV (over 6 kV) cable networks the attenuation, noise and coupling efficiency, as shown by the experience of the authors, are most important. The PLC transmission problems in low-voltage networks are recognized and fairly widely analysed and known in the literature [1], [7]–[12]. In networks, whereas of medium voltage (above 6 kV) both the overhead as especially cable underground (mining), this question is relatively little researched and reported [9] and [17]. It is mainly due to limited access for testing to verify the developed theories. From the research conducted by the authors it is shown that the efficiency of high frequency transmission (BPL) in cable mine networks is subjected to significant changes depending on the network conditions (without supply, under voltage but un-loaded, loaded) and this is not necessarily caused by noise (the bridged influence of energy receivers can be made negligible here). However, this is subject to further research and analysis in this area. It should be emphasized that the capacitive coupling in medium voltage cable networks is not recommended due to safety risk. The coupler must be connected solidly to a given phase/phases without any short-circuit protection (fuse). It makes a potential risk of equipment damage in the case of any ground fault. Therefore, the only way here is to connect the coupler directly to the bus/phase, but by means of a tiny electric wire of a length sufficient to meet requirements of electrical strength in a case of its burning.

The objective of this paper is to approach theoretically and experimentally the BPL (2 MHz–32 MHz) transmission efficiency in existing 6 kV cable lines of selected underground mine. It is followed by the derivation of the power line parameters using the transmission line theory. A sample mine network was adapted to verify the validity of this theoretical considerations through practical measurements.

II. SELECTED CABLE NETWORK STRUCTURE FOR BPL IMPLEMENTATION

To implement the BPL technology a radial cable network (that simplified diagram is presented in Fig. 1) has been selected. It is characterized by significant distortion of current waveforms due to powering of converters especially hoisting machines. Moreover, some part of the cable (about 1100 m) is located inside a mine shaft making the installation of the additional couplers for repeaters impossible.
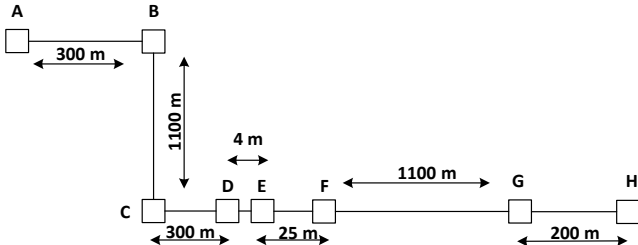

Fig. 1. Selected 6 kV cable line structure for BPL implementation.

The transmission quality was found to be significantly changed with time. It can be compared from Fig. 2 for measured SNR value for unloaded cable (for section of the A-B and B-C). The section B-C broadcast is seen practically ineffective (it is also suspected that some negative impact has the value of the ambient temperature). Therefore, in order to explain the reasons for the deterioration of the transmission efficiency the need arose to develop appropriate analytical model based on transmission line theory.
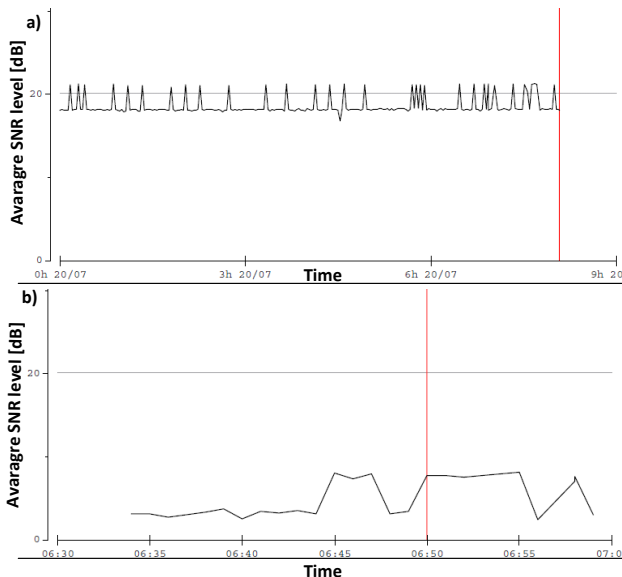

Fig. 2. The measured average value of SNR as a function of time for the cable segment A-B (a); and segment B-C (b), located on the surface and in the mine shaft respectively (channel bandwidth 2 MHz–7 MHz, 1536 orthogonal carriers, TDD, cables without load).

III. ANALYSIS OF THE TRANSMISSION EFFICIENCY

A section of the cable network A-B with a length of approximately 300 m located on the surface of the mine was selected for the theoretical analysis of the problem and practical verification (Fig. 1). It was imposed on the practical possibilities of couplers installation such as inductive and capacitive and the practical aspects of testing. Our goal was to determine first of all the characteristic

impedance Z_0 and the propagation constant of the 3-phase cable conductor modelled as a transmission line. These parameters dominate the wave behaviour along the line.

A. Power 3-Phase Cable Modelling

The cable under study is the 3-phase mine cable (type YKGYFtZmyn 3 mm × 185 mm) with central copper screen and equipped with steel armour to protect it mechanically as indicated in Fig. 3. The L1, L2 and L3 phases separated uniformly each other are made up of stranded copper conductors with PVC insulation. The two intrinsic cable parameters for the transmission line, i.e. the characteristic impedance Z_0 and the propagation constant Υ can be calculated by (1), (2) [4], [13] and [14]:

$$z_0 = \sqrt{\frac{R + j\omega L}{G + j\omega C}}, \qquad (1)$$

$$\gamma = \alpha + j\beta = \sqrt{(R + j\omega L)(G + j\omega C)}, \qquad (2)$$

where ω is the angular frequency, the real part α and the imaginary part β of the propagation constant are the attenuation constant and phase constant respectively. In order to facilitate the comparison of calculation results with the measurements the α coefficient expressed in dB/m.

The electrical parameters of the cable have been derived therefore, basing on the knowledge of the cable structure, the cross-sectional geometrical dimensions and properties of the materials used as electrically conductive or insulating (Fig. 3).
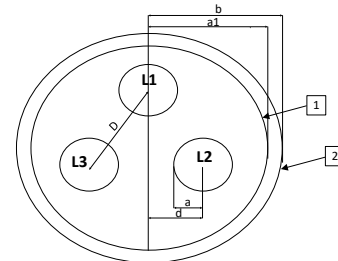

Fig. 3. Cross-sectional view of the 3-phase 6 kV power cable.

Resistance has been calculated taking into account the skin effect in the conductors, screen as well as in armour. The skin depth (δ) is a function of frequency (f) and can be calculated using the (3) [4], [13], [14]

$$\delta = \sqrt{\frac{1}{\pi \times f \times \mu_c \sigma_c}}, \qquad (3)$$

where σ_c and μ_c are the conductivity and permeability of the conductor respectively.

Analysed the structure of the 3-phase cable, the resistance of one solid phase can be calculated as follows [4], [13], [14]

$$R_{solid} = \frac{1}{\pi \times a \times \delta \times \sigma_c}, [\Omega / m], \qquad (4)$$

where a is the radius of the conductor.

However, taking into account the reduction of the resultant cross-section of the phase due to the wiring

stranding a correction factor X_R must be included. It is given by (5) [4] and [13]

$$X_R = \\ = \frac{\cos^{-1}\left(\frac{r_{wire} - \delta}{r_{wire}}\right) \times r_{wire}^2 - (r_{wire} - \delta)^2 \sqrt{r_{wire}^2 - (r_{wire} - \delta)^2}}{2 \times r_{wire} \times \delta}, \quad (5)$$

where r_{wire} is the radius of a single wire in the stranded conductor, δ is the skin depth. With this correction, (6) gives the resistance for the single phase as following

$$R = X_R \times R_{solid}, \left[\Omega / m\right], \quad (6)$$

Thus, the final resistance for the 3-phase cable is equal to

$$R_{cable} = \frac{R}{3}. \quad (7)$$

In the case of considering the effects of the screen R_{screen} and the armor R_{armor} their resistance values were calculated from (4). For the screen however, a_1 is its radius, whereas, for the armor must be taken into account both its different radius (b) as well as the magnetic permeability of iron. The resultant resistance R_T of the 3-phase power cable constitutes therefore, the parallel connection of all components calculated as follows

$$\frac{1}{R_T} = \frac{1}{R_{Cable}} + \frac{1}{R_{Screen}} + \frac{1}{R_{Armor}}, \quad (8)$$

where

$$R' = \frac{R_{Cable} \times R_{Screen}}{R_{Cable} + R_{Screen}}. \quad (9)$$

As a result, the resultant unit resistance of the cable in the function of the frequency doesn't increase, as expected for the phase conductors due to the skin effect, but decreases (as it can be seen from further consideration of the authors).

The inductance of the 3-phase power cable includes the self-inductance of particular phase conductors L_s and the mutual inductance L_m between them and the self inductance of the armor L_a as shown in Fig. 4.
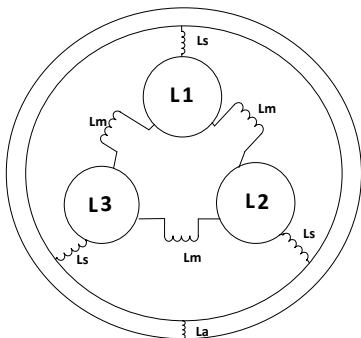

Fig. 4. Equivalent inductance diagram in 3-phase power line.

From [4], [13], [14] the self inductance for one phase conductor is given by (10)

$$L_s = \frac{\mu_c}{8\pi}, \left[H/m\right], \quad (10)$$

and the mutual inductance between a pair of parallel conductors is

$$L_m = \frac{\mu_c}{\pi} \cosh^{-1}\left(\frac{D}{2a}\right), \left[H/m\right]. \quad (11)$$

The self inductance of the armour can be derived from (12)

$$L_a = \frac{\mu_a}{2\pi} \ln\left(\frac{b}{a}\right), \left[H/m\right], \quad (12)$$

where μ_a is the permeability of the armour material.

The resultant inductance L_w of the cable without armour is (Fig. 5)

$$L_w = 3L_s + \frac{L_m}{3}, \quad (13)$$

whereas, after taking into account the armour it becomes L_c (Fig. 6)

$$L_c = \frac{(L_w \times L_a)}{(L_w + L_a)}. \quad (14)$$

The resultant capacity of the cable includes the phase-to-phase capacitance C_{cable}, the capacitance between particular phases and the screen $C_{coaxial}$ and between the screen and armor C_a (it can not be ignored as results from authors' investigations) as indicated in Fig. 6.
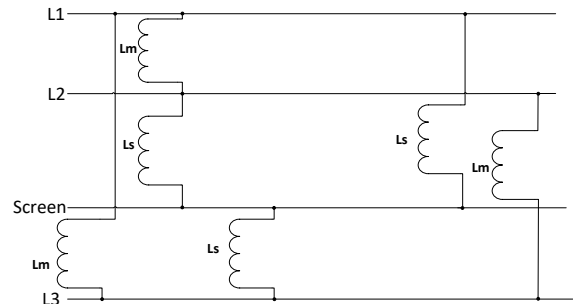

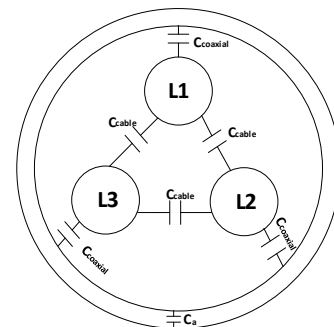Fig. 5. Resultant inductance of the 3-phase MV cable without the armour.

Fig. 6. Equivalent capacitance diagram in 3-phase power cable.

The phase-to phase capacitance can be calculated as shown in (15) and (16)

$$C_{cable} = \frac{\pi\varepsilon}{\cosh^{-1}\left(\dfrac{D}{2a}\right)}, [\text{F/m}], \qquad (15)$$

where D is the distance between the centers of the phase conductors, a is the radius of the phase conductor, ε is the permittivity of the dielectric material in between the conductors.

The determination for $C_{coaxial}$ and C_a was found as for the coaxial cylindrical conductors [13]–[15]

$$C_{coaxial} = \frac{2\pi\varepsilon}{\ln\left(\dfrac{b}{a}\right)}, [\text{F/m}], \qquad (16)$$

where a_1 – the radius of the cable to the screen.

$$C_a = \frac{2\pi\varepsilon}{\ln\left(\dfrac{b_1}{a_1}\right)}, [\text{F/m}]. \qquad (17)$$

Using the transformation for the star-delta connection the total capacitance diagram is derived as in Fig. 7, where

$$C'_{cable} = \frac{C_{cable}}{3}. \qquad (18)$$

Considering that:

$$C' = \frac{C_{Coax} \times C'_{cable}}{C_{Coax} + C'_{cable}}, \qquad (19)$$

$$C_w = 3 \times C', \qquad (20)$$

the resultant capacitance C of the 3-phase power cable is given as

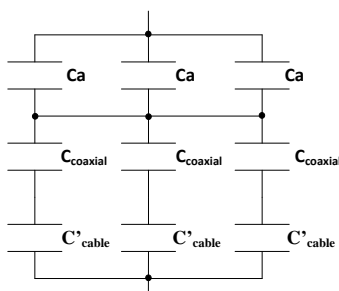$$C = \frac{(3C_a \times C_w)}{(3C_a + C_w)}. \qquad (21)$$

Fig. 7. Total capacitance of the 3-phase power cable.

If the medium has the same space dependence or if the medium is homogeneous (like in the MV power cable) the following equation for the cable conductance holds [4]

$$G = \frac{\sigma \times C}{\varepsilon}, [\text{S/m}], \qquad (22)$$

where σ is conductivity of the dielectric material, ε is the dielectric constant and C is resultant capacitance of the cable.

For the inductive coupling (of all 3 phases of the cable), all electrical parameters of the cable were modelled and calculated in accordance with (1)–(22). However, in case of the capacitive coupling (of one of the phases with the ground), it was necessary to omit the influence of the armour and the screen. Therefore, simplifying the calculation, the cable resistance was derived from (9), the capacitance from (20) and the conductivity from (22) respectively. However, in this last case $C = C_W$.

B. Results and Discussion

Having derived all the primary parameters of the 3-phase power cable (Table I) its characteristic impedance and propagation constant were able to be obtained. From the calculated results it is seen that the impedance value is changed with the frequency however, this relationship is non-linear and depends on way of coupling. The dependence of the characteristic impedance of the analysed cable on the frequency (2 MHz–30 MHz) shows that above 7.5 MHz the impedance value is more less constant and quite close to the matching value equal to around 50 Ω (Fig. 8(a)). The phase and group delay however, for inductive coupling do not change with frequency. On the contrary, when use the capacitive coupling, the group delay increases 4 times (Fig. 8(d)). The phase shift increases linearly with frequency (Fig. 8(c)) as well. The cable resistance indicates also the increase with frequency (Fig. 8(b)) what is manifested by the increased attenuation value with the cable length (Fig. 9).

TABLE I. CABLE PARAMETERS.

Dimensions		Physical parameters	
a [mm]	15	$\sigma_c \left\lfloor \dfrac{1}{nm} \right\rfloor$	$17,24 \cdot 10^9$
D [mm]	46,96	$\sigma_a \left\lfloor \dfrac{1}{nm} \right\rfloor$	$10,02 \cdot 10^6$
b [mm]	63	$\sigma \left\lfloor \dfrac{1}{nm} \right\rfloor$	10^{14}
a1 [mm]	55	ϵ	3,3
d [mm]	23,48	μ_c	0,9999
		μ_a	60

The attenuation as a function of distance, presented in Fig. 9, have been calculated for the average frequency from the range of 2 MHz–30 MHz, taking into account the number of subcarriers (1536). Having the specified theoretical parameters of the transmission channel, the most favourable frequency range of the signal (mode) can be selected. For the analysed 6 kV cable, it seems that the frequency of the entire analysed band (2 MHz–30 MHz) can be used, taking into account the impedance matching. However, considering the increase in attenuation with the frequency, authors carried out tests using the mode of the lowest frequency equal to 2 MHz–7 MHz respectively. In this respect, however, there is found a quite significant impedance mismatching. This can be clearly seen when analyse in detail the parameters of the transmission channel for the selected mode (2 MHz–7 MHz). As shown in Fig. 10, the characteristic impedance decreases

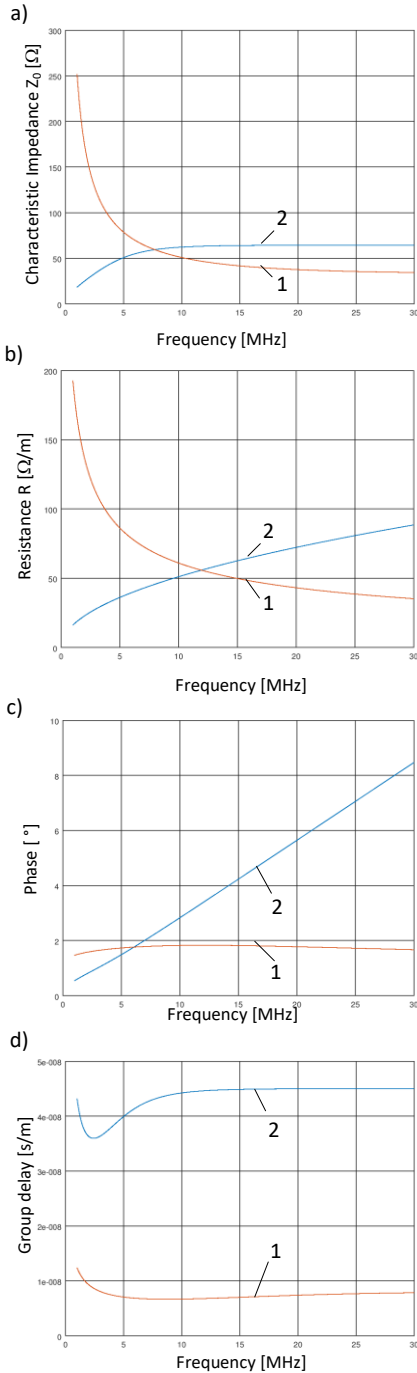exponentially from about 100 Ω to about 83 Ω with the analysed frequency.

a)

b)

c)

d)

Fig. 8. The calculated values of the characteristic impedance a); unit resistance b); signal phase c); and group delay d) as a function of frequency from 2 MHz to 30 MHz (1 – inductive coupling, 2 – capacitive coupling).
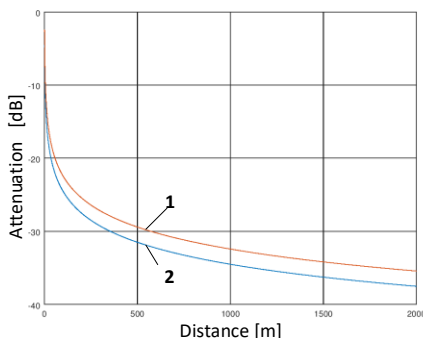

Fig. 9. Variation of an attenuation with the cable length for inductive (1) and capacitive coupling (2).
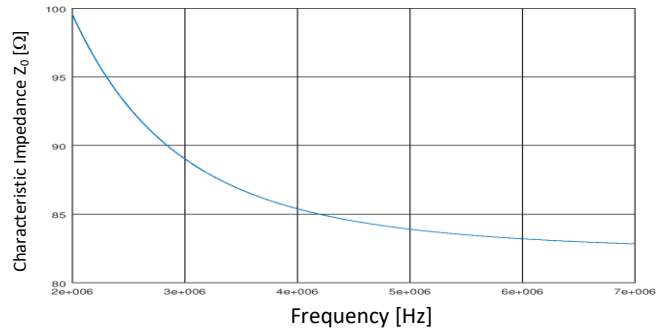

Fig. 10. The calculated values of the characteristic impedance of the analysed cable; as a function of frequency from 2 MHz to 7 MHz.

As a result, the modelled transmission channel is misaligned with the conditions of operation. This has been confirmed by the measurement results what for SNR, for the analysed cable length of approximately 300 m is shown as an example in Fig. 11.
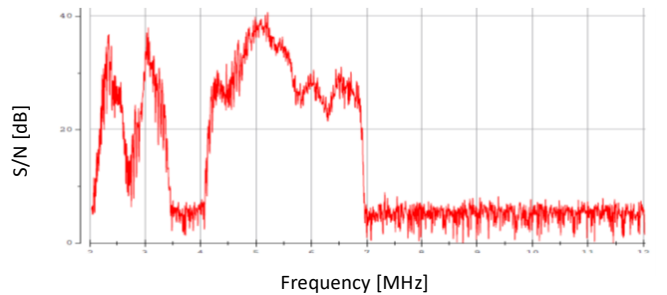

Fig. 11. Variation of measured value of the instantaneous SNR with frequency.

It can be seen clearly that the transmission efficiency is highest here, in the range of just from 4 MHz (to 7 MHz) and not, as would seem intuitively from 2 MHz. Very important from the point of view of the transmission efficiency is the analysis of variation of both attenuation and phase constant with frequency. The attenuation is related to the unit resistance value of the power cable, which in turn depends on the frequency and decreases almost 2-times for the analysed transmission channel of 2 MHz–7 MHz. The derived cable attenuation therefore, decreases linearly within the analysed range of frequencies not exceeding 0.2 dB/m (Fig. 12).
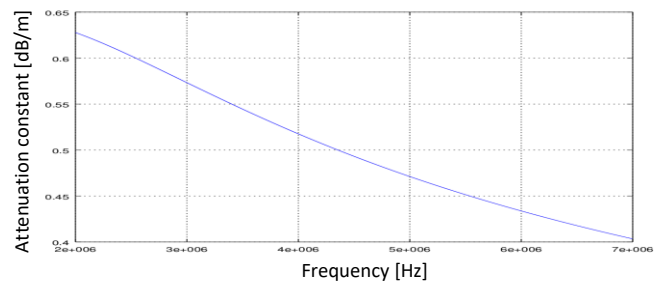

Fig. 12. Derived attenuation constant versus frequency.

One has to take into account, that deterioration of the transmission quality results not only from the increase in the attenuation but is also due to the changes in the phase constant versus frequency. For the cable under test the derived phase constant was found to change linearly and increases almost 3-times (It can result in PLC-BPL signal fading due to potential subtraction the OFDM subcarriers (1536 subcarriers). The group delay (τ) which represents

the time needed for a signal to travel 1m is found to be relatively low (about 0.4 µs/m) and practically not rise above 6 MHz

$$\tau = \frac{d\beta}{d\omega}. \tag{23}$$

Due to the anticipated application of BPL for the cable length of around 2 km the appropriate recalculation for the inductive coupling were performed for the attenuation, phase shift and group delay of the signal as a function of length. In order to make the calculations first attenuation value was averaged for all 1536 sub-carriers of the OFDM transmission channel, and then was respectively converted to obtain the attenuation as a function of cable length.

The derived data show that the value of cable attenuation increases exponentially with its length, with the largest increase in attenuation in the range of up to 500 m. The group delay of the signal increases linearly with the length of the cable and at a distance of approximately 500 m reaches almost 7.5 µs. The group delay is related to the phase change, which is also found to be practically linear (for 500 m reaches about 40 degrees) (Fig. 13).
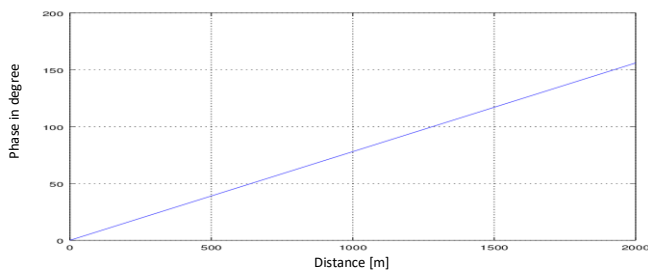

Fig. 13. Derived variation of the signal phase with the cable length.
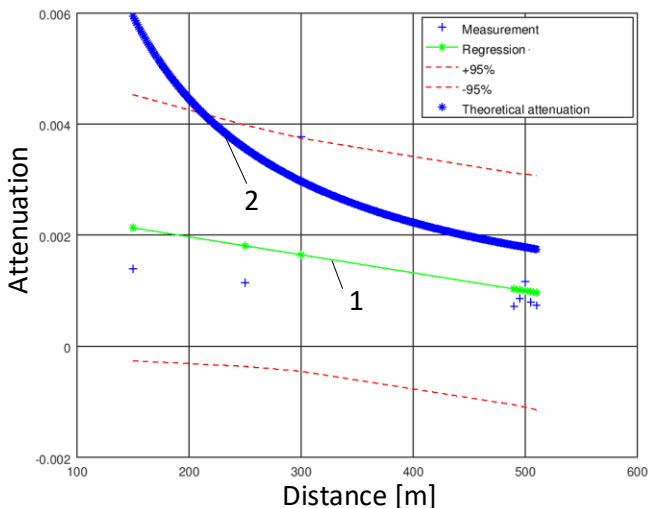

Fig. 14. Comparison of measured and derived values of attenuation as a function of length; 1 – regression, 2 – theoretical.

They showed fairly good agreement with the theoretical values (with an accuracy of =+/- 10 % for a length of up to 500 m). However, it must be noted that the difference in calculated values for smaller from about 250 m of the cable length results from the fact of application of the long line theory (far field). For the applied frequency range (2 MHz–7 MHz) it should be rather verified by the near field approach what was confirmed by further authors investigations.

IV. CONCLUSIONS

In order to ensure the effective BPL transmission in the cable MV network of underground mine the propagation conditions for a given frequency range should be respectively specified and recognized. This requires first of all determination of the characteristic impedance value and its relationship with frequency as well as variation of the damping coefficient and the phase constant as a function of frequency and the length of the cable line. Using the long-line theory for the structure and parameters of the selected 3-phase cable, it was possible to calculate the necessary cable parameters affecting the transmission quality. The results show that the typical cable parameters vary in different ways along with the frequency of the signal PLC-BPL and the length of the transmission line. They have been verified by measurements for the analysed line showing a pretty big coincidence from practical point of view (+/-10 %). From the tests performed on the object in the mine for frequency 2 MHz–7 MHz it was found that for the particular 3-phase cable the transmission channel of a different bandwidth should be used. Therefore, prior to the BPL implementation, and selection of the way of coupling, as well as the mode frequency, one has to carefully estimate the attenuation coefficient, the phase constant as well as the group delay of the signal depending on the frequency of the channel and the type and length of the cable. In other words, the physical properties of the transmission channel prior to implementation should be recognized based on the methodology proposed in the article.

REFERENCES

[1] X. Carcelle, *Power line communications in practice*. Artech House, 2009.
[2] D. Pyda, M. Habrych, K. Rutecki, B. Miedzinski, "Analysis of narrow band PLC technology performance in low-voltage network", *Elektronika ir Elektrotechnika*, vol. 20, no. 5, 2014. DOI: 10.5755/j01.eee.20.5.7101.
[3] P. Mlynek, J. Misurec, M. Koutny, "Random channel generator for indoor power line communication", *Measurement Science Review,* vol. 13, no. 4, pp. 206–213, 2013. DOI: 10.2478/msr-2013-0032.
[4] H. Meng *et al.*, "Modeling of transfer characteristics for the broadband power line communication channel", *IEEE Trans. Power Deliv.*, vol. 19, no. 3, pp. 1057–1064, 2004. DOI: 10.1109/TPWRD.2004.824430.
[5] J. N. Murphy, H. E. Parkinson, "Underground mine communications", in *Proc. IEEE*, vol. 66, no. 1, pp. 26–50, 1978. [Online]. Available: https://www.cdc.gov/niosh/mining/works/coversheet164.html
[6] A. Milioudis, G. Andreou, D. Labridis, "Optimum transmitted power spectral distribution for broadband power line communication systems considering electromagnetic emissions", *Electr. Power Syst. Res.*, vol. 140, pp. 958–964, 2016. DOI: 10.1016/j.epsr.2016.03.047.
[7] G. Prasad, L. Lampe, S. Shekhar, "In-band full duplex broadband power line communications", *IEEE Trans. Commun.*, vol. 64, no. 9, pp. 3915–3931, 2016. DOI: 10.1109/TCOMM.2016.2587284.
[8] F. Zwane, T. J. O. Afullo, "An alternative approach in power line communication channel modelling", *Prog. Electromagn. Res. C*, vol. 47, pp. 85–93, 2014. DOI: 10.2528/PIERC13121303.
[9] A. G. Lazaropoulos, "Broadband transmission characteristics of overhead high-voltage power line communication channels", *Prog. Electromagn. Res. B*, vol. 36, pp. 373–398, 2012. DOI: 10.2528/PIERB11091408.
[10] J. Dickinson, P. J. Nicholson, "Calculating the high frequency transmission line parameters of power cables", in *Proc. IEEE Int. Symp. Power Line Communications and its Applications*, pp. 127–133, 1997.
[11] P. A. Brown, "Identifying some techno-economic criteria in PLC/BPL applications and commercialization", *IEEE Int. Symposium on Power Line Communications and Its Applications*, 2005, pp. 234–239. DOI:

10.1109/ISPLC.2005.1430504.

[12] Y. Xiao, J. Zhang, F. Pan, Y. Shen, "Power line communication simulation considering cyclostationary noise for metering systems", *J. Circuits, Syst. Comput.*, vol. 25, no. 9, p. 1650105, 2016. DOI: 10.1142/S021812661650105X.

[13] Cheng, D.K. "Fundamentals of engineering electromagnetics",. Cheng, D.K. "Field and wave electromagnetics." Addison-Wesley, Jan. 1989.

[14] D. M. Sheen, S. M. Ali, D. E. Oates, R. S. Withers, J. A. Kong, "Current distribution, resistance, and inductance for superconducting strip transmission lines", *IEEE Trans. Appiled Supercond.*, vol. 1, no. 2, pp. 108–115, 1991. DOI: 10.1109/77.84617.

[15] A. Milioudis, G. Andreou, D. Labridis, "Optimum transmitted power spectral distribution for broadband power line communication systems considering electromagnetic emissions", *Electr. Power Syst. Res.*, vol. 140, pp. 958–964, 2016. DOI: 10.1016/j.epsr.2016.03.047.